Molecular Immunology 127 (2020) 79–86

Contents lists available at ScienceDirect

Molecular Immunology

journal homepage: www.elsevier.com/locate/molimm

Cross-reactivity of mouse IgG subclasses to human Fc gamma receptors: Antibody deglycosylation only eliminates IgG2b binding

A. Robin Temming [a], Arthur E.H. Bentlage [a], Steven W. de Taeye [a,b], Gerlof P. Bosman [c], Suzanne N. Lissenberg-Thunnissen [a], Ninotska I.L. Derksen [b], Giso Brasser [d], Juk Yee Mok [d], Wim J.E. van Esch [d], Heather L. Howie [e], James C. Zimring [e], Gestur Vidarsson [a,*]

[a] Department of Experimental Immunohematology, Sanquin Research and Landsteiner Laboratory, Amsterdam University Medical Center, University of Amsterdam, Amsterdam, The Netherlands
[b] Department of Immunopathology, Sanquin Research and Landsteiner Laboratory, Amsterdam University Medical Center, University of Amsterdam, Amsterdam, The Netherlands
[c] Department of Chemical Biology and Drug Discovery, Utrecht Institute for Pharmaceutical Sciences, Utrecht University, Utrecht, The Netherlands
[d] Sanquin Reagents, Amsterdam, The Netherlands
[e] Department of Pathology, Carter Immunology Center, University of Virginia School of Medicine, Charlottesville, Virginia, United States

ARTICLE INFO

Keywords:
Human Fc gamma receptor
Mouse IgG subclass
Surface plasmon resonance
Affinity
Cross-reactivity
Deglycosylation

ABSTRACT

Immunoglobulin G (IgG) antibodies are important for protection against pathogens and exert effector functions through binding to IgG-Fc receptors (FcγRs) on myeloid and natural killer cells, resulting in destruction of opsonized target cells. Despite interspecies differences, IgG subclasses and FcγRs show substantial similarities and functional conservation between mammals. Accordingly, binding of human IgG (hIgG) to mouse FcγRs (mFcγRs) has been utilized to study effector functions of hIgG in mice. In other applications, such as immunostaining with mouse IgG monoclonal antibodies (mAbs), these cross-reactivities are undesired and prone to misinterpretation. Despite this drawback, the binding of mouse IgG (mIgG) subclasses to human FcγR (hFcγR) classes has never been fully documented. Here, we report detailed and quantifiable characterization of binding affinities for all mIgG subclasses to hFcγRs, including functional polymorphic variants. mIgG subclasses show the strongest binding to hFcγRIa, with relative affinities mIgG2a = mIgG2c > mIgG3 >> mIgG2b, and no binding by mIgG1. hFcγRIIa/b showed general low reactivities to all mIgG (mIgG1> mIgG2a/c > mIgG2b), with no reactivity to mIgG3. A particularly high affinity was observed for mIgG1 to the hFcγRIIa-R131 polymorphic variant. hFcγRIIIa showed lower binding (mIgG2a/c > mIgG3), slightly favouring binding to the hFcγRIIIa-V158 over the F158 polymorphic variant. No binding was observed of mIgG to hFcγRIIIb. Deglycosylation of mIgG1 did not abrogate binding to hFcγRIIa-R131, nor did deglycosylation of mIgG2a/c and mIgG3 prevent hFcγRIa binding. Importantly, deglycosylation of the least cross-reactive mIgG subclass, mIgG2b, abrogated reactivity to all hFcγRs. Together, these data document for the first time the full spectrum of cross-reactivities of mouse IgG to human FcγRs.

1. Introduction

Immunoglobulins (Ig) play a pivotal role in adaptive immune responses and are produced and secreted by plasma B cells. Each Ig molecule has a dimeric structure with two antigen-binding fragment (Fab) domains symmetrically linked via the hinge region to one crystallizable fragment (Fc) domain. This Fc portion enables antibodies to exert effector functions like activation of the complement system through interaction with C1q, or activation of myeloid and natural killer (NK) cell-mediated effector functions through IgG-Fc receptors (FcγRs).

Immunoglobulins comprise several classes (IgM, IgD, IgA, IgE, IgG) of which IgG make up the main fraction in serum and can, in humans, be further divided into IgG1, IgG2, IgG3 and IgG4. These IgG subclasses show highly conserved amino acid sequences (more than 90% homology) (Vidarsson et al., 2014) but each having its unique functional characteristics, e.g. acting through different FcγRs (de Taeye et al.,

* Corresponding author at: Department of Experimental Immunohematology, Sanquin Research and Landsteiner Laboratory, Amsterdam University Medical Center, University of Amsterdam, Plesmanlaan 125, 1066 CX Amsterdam, The Netherlands.
E-mail address: G.Vidarsson@sanquin.nl (G. Vidarsson).

https://doi.org/10.1016/j.molimm.2020.08.015
Received 11 March 2020; Received in revised form 14 August 2020; Accepted 24 August 2020
Available online 15 September 2020

2019; Vidarsson et al., 2014). This seems to arise directly from the differential binding affinity of the IgG subclasses to different FcγRs (Bruhns et al., 2009; Vidarsson et al., 2014). In mice, similar to humans, IgG make up the main antibody serum fraction and can be divided into four subclasses (IgG1, IgG2a, IgG2b, IgG3). However, some strains of mice express IgG2c instead of IgG2a (e.g. in C57BL/6 mice), likely as an allotypic variation (Martin et al., 1998).

FcγRs are expressed on the surface of different cell types, including myeloid and NK cells, and consist of activating FcγRIa, FcγRIIa, FcγRIIc and FcγRIIIa, inhibitory FcγRIIb, and the glycosylphosphatidylinositol-linked FcγRIIIb (Bruhns, 2012). FcγR polymorphisms influence IgG-FcγR interactions (Boesch et al., 2017; Bruhns et al., 2009; Dekkers et al., 2017a; van der Pol and van de Winkel, 1998). Illustrative for this are the FcγRIIa polymorphic variants having either a histidine (H) or an arginine (R) residue at position 131. This amino acid difference causes a substantial change in affinity towards IgG, especially IgG2 (~5-fold difference) (Bruhns et al., 2009; Dekkers et al., 2017a). For FcγRIIIa the valine (V)/phenylalanine (F) 158 and for FcγRIIIb the NA1/NA2 polymorphism can be found which also determine IgG binding strength (Boesch et al., 2017; Bruhns et al., 2009; Dekkers et al., 2017a). In addition, IgG-FcγR interactions also depend on both the presence and the exact composition of the conserved *N*-linked glycan in the IgG-Fc (Bruggeman et al., 2017; Bruhns et al., 2009; Dekkers et al., 2017b; Falconer et al., 2018; Lippold et al., 2019; Subedi and Barb, 2016). Furthermore, FcγRIIIa/b *N*-linked glycosylation has also been demonstrated to affect IgG binding capacity (Dekkers et al., 2018; Falconer et al., 2018; Ferrara et al., 2011; Subedi and Barb, 2018).

Due to the functional co-evolution of the FcγR and IgG protein families, it is not surprising that interspecies cross-reactivities occur. Human IgG (hIgG) subclasses are known to interact well with mouse FcγRs (mFcγRs) and to those of cynomolgus monkeys (Dekkers et al., 2017a; Derebe et al., 2018), warranting their use in animal models. Conversely, mouse IgG (mIgG) subclasses also bind to human FcγRs (hFcγRs), but this has been less thoroughly studied. To illustrate, most available studies reported binding abilities or relative affinities of one specific or a selection of mIgG subclasses to hFcγR types expressed on immune cells or on cell lines (Jones et al., 1985; Jönsson et al., 2011; Lubeck et al., 1985; Mancardi et al., 2013; Miller et al., 1996; Parren et al., 1992). These studies together do not cover the full spectrum of mIgG-hFcγR interactions and inter-study comparison is complicated by differences in experimental approach, antibody formulation and hFcγR context. To our knowledge, only few studies reported exact affinity values as determined by surface plasmon resonance imaging (SPRi) or ligand binding assays, but these were limited to mIgG2a binding to hFcγRIa and hFcγRIIIa/b (Mancardi et al., 2013; Miller et al., 1996). This lack of detailed knowledge is striking as multiple diagnostic, fundamental and translational research platforms rely heavily on the use of monoclonal antibodies (mAbs), e.g. immunostaining and immunodetection, of which most are of mouse origin. In addition, in hFcγR transgenic mouse models endogenous mIgG is present and murine mAbs are often used to understand mIgG-hFcγR interactions. Therefore, a full side-by-side and quantifiable characterization of these cross-reactivities is of crucial importance for the completeness of fundamental knowledge and in particular useful for future practice.

Functionally, mIgG have been demonstrated to trigger effector functions through FcγRs in a human context (Kipps et al., 1985; Meinderts et al., 2017), e.g. human neutrophils efficiently phagocytose erythrocytes opsonized with mIgG1. Despite knowing that mIgG1 efficiently interacts with hFcγRIIa, particularly of the R131 allotypic variant (Parren et al., 1992; Warmerdam et al., 1991), we generally do not know exactly which mIgG subclasses interact with hFcγR as studies published to date are incomplete, lack information on all hFcγRs and/or do not include all known mIgG subclasses (Jönsson et al., 2011; Lubeck et al., 1985; Mancardi et al., 2013; Miller et al., 1996; van der Pol and van de Winkel, 1998). To circumvent interspecies IgG-FcγR cross-reactivity properly, tools have been developed, such as generation of Fab or $F(ab')_2$ fragments. More recently, even more simplified tools have been developed, e.g. enzymatic digestions (e.g. using *Streptococcus pyogenes* endoglycosidase S [EndoS], which hydrolyses IgG *N*-linked glycans leaving the primary *N*-acetylglucosamine) to make deglycosylated mAbs (Collin and Olsén, 2001; Lux et al., 2013) which generally lose their affinity for FcγRs probably because they adopt a closed conformation between the two IgG-Fc-CH2 domains preventing FcγR binding (Feige et al., 2009). While these mAbs are generally believed to have still some residual hFcγRIa binding (Lux et al., 2013), no comprehensive experimental evidence exists for binding affinities of deglycosylated mIgG subclasses for hFcγR.

A persisting misconception is that background FcγR binding by mAbs can simply be corrected for using isotype controls. However, isotypes are aspecific and therefore unable to simulate *in cis* interactions through Fab and Fc regions occurring simultaneously. These interactions stabilize antibody binding through concurrent antigen and FcγR binding (Kurlander effect) resulting in underestimation of background signals and publication of false positive results (Hogarth and Pietersz, 2012; Kurlander, 1983; MacIntyre et al., 1989, 1988; Saeland et al., 2001). This emphasizes the importance of using mAbs with an inactive or removed Fc domain when studying FcγR-expressing cells.

In order to provide a complete overview of cross-reactivities and to understand the potential interference in diagnostic tests, we performed a detailed binding profile for all mIgG subclasses, with or without EndoS treatment, to the complete hFcγR panel, including all known functional extracellular hFcγR polymorphisms, using a state-of-the-art SPRi-based biosensor platform.

2. Materials and methods

2.1. Amino acid sequence alignments

Alignment of mIgG-/hIgG-Fc-CH2-CH3 and mFcγR/hFcγR extracellular domain amino acid sequences have been performed using the online blastp suite-2sequences tool (Altschul et al., 2005, 1997). Amino acid sequences were derived from UniProt database with entries: P01857 (hIgG1), P01859 (hIgG2), P01860 (hIgG3), P01861 (hIgG4), P01868 (mIgG1), P01863 (mIgG2a), P01867 (mIgG2b), A0A0A6YY53 (mIgG2c), P03987 (mIgG3) for IgG subclasses and P12314 (hFcγRIa), P12318 (hFcγRIIa), P31994 (hFcγRIIb), P31995 (hFcγRIIc), P08637 (hFcγRIIIa), O75015 (hFcγRIIIb), P26151 (mFcγRI), P08101 (mFcγRIIb), P08508 (mFcγRIII), A0A0B4J1G0 (mFcγRIV) for FcγRs.

2.2. Recombinant EndoS production

A PCR product of *Streptococcus pyogenes* EndoS cDNA (GenBank: AAK00850.1, amino acids 37-995) was generated using primers from Integrated DNA Technologies: 5'-CCAGGATCCTGGATCTGAGGAGAAGACTGTTCAGGTTCAG-3' and 5'-CTCTTTTCCGTCGACGATTTTTTTGAGCTCCGAATTAATTGG-3'. After PCR product clean-up, the amplicon was digested (BamHI/XhoI), purified and ligated into a pET47b + bacterial vector (EMD Millipore) incorporating a 6xHis-tag to the sequence. After DH5α transformation and subsequent extraction of the plasmid, the insertion was confirmed by sequencing. Next, BL21(DE3) *E. coli* competent cells (New England Biolabs) were transformed with the EndoS-encoding pET47b + vector, a colony was picked, expanded at 37 °C, induced with 1 mM isopropyl-beta-D-thiogalactopyranoside (Thermo Scientific) and cultured overnight at 20 °C. Then, cells were pelleted at 3,000 g, resuspended in lysis buffer (5% of culture volume), incubated at 37 °C for 1 hour and sonicated for 30 minutes on ice. After centrifugation at 10,000 g, clear supernatant was loaded onto a gravity flow 4 ml Ni-NTA column (GE Life Sciences). Once washed, EndoS was eluted in buffer (50 mM TRIS-HCl and 250 mM NaCl pH 8) supplemented with 250 mM imidazole (Sigma-Aldrich). The eluate was concentrated using Vivaspin 6 filter tubes (MWCO 30 kDa) (Sartorius) and purified on a PBS equilibrated Superdex 200 Increase 10/300 G L

column (GE Life Sciences) attached to a Shimadzu Nexera system. Before application, EndoS activity was confirmed by liquid chromatography–mass spectrometry based on the hydrolysis of purified sialylglycopeptide (Liu et al., 2017).

2.3. Antibody production and preparation

Monoclonal hIgG1 with specificity for Rhesus D were produced as previously described, with the only adaptation that PEImax was used as a transfection reagent (Dekkers et al., 2017a; Vink et al., 2013; Temming et al., 2019). Similarly, a panel of monoclonal mIgG subclasses with specificity for the Kell blood group K antigen (PUMA1) were generated as described previously (Dekkers et al., 2017a; Howie et al., 2016). After antibody isolation, IgG-containing fractions were concentrated by centrifugation using Amicon Ultra centrifugal filter units (MWCO 10 kDa) (Merck, Millipore) and overnight buffer-exchanged to PBS through dialysis. Before application IgG formulations were confirmed aggregation-free by high performance liquid chromatography (HPLC) using a Superdex 200 increase 10/300 G L column (GE Life Sciences) in combination with multi angle light scattering (miniDAWN, Wyatt) and differential refractive index (Optilab, Wyatt). IgG deglycosylation was performed through enzymatic glycan digestion by incubating formulations in PBS for 2 hours with recombinant EndoS at 37 °C in an enzyme:substrate ratio of 1:20. Glycan removal was confirmed by sodium dodecyl sulfate-polyacrylamide gel electrophoresis (SDS-PAGE), as described in the next section.

2.4. SDS-PAGE

Purified antibody (3 μg) or EndoS (0.3 μg) samples were diluted in demineralized water to a total volume of 15 μl. To prepare denatured protein samples, 5 μl of 4x NuPAGE LDS sample buffer (Invitrogen), supplemented with 1:100 β-mercaptoethanol, was added and samples were then incubated at 95 °C for five minutes. Subsequently, each slot of a NuPAGE 4 to 12% Bis-Tris Protein gel (12 wells; Invitrogen) was loaded with 20 μl of denatured protein sample, 20 μl 1x sample buffer, or 5 μl PageRuler Plus Prestained Protein ladder (Thermo Scientific). After sample loading, gels were run in 1x 3-(N-morpholino) propanesulfonic acid buffer for 55 minutes at a constant voltage of 200, and a starting current of 100 mA which was increased to 125 mA after 15 minutes. After running, gels were washed twice with demineralized water for 10 minutes, then stained with Blue Silver solution (Candiano et al., 2004) for 2 hours and eventually destained overnight in demineralized water.

2.5. Human FcγR production

C-terminally biotinylated human hFcγRIIa-H131 (10374-H27H1-B), hFcγRIIa-R131 (10374-H27H-B), hFcγRIIb (10259-H27H-B), hFcγRIIIa-F158 (10389-H27H-B) and 10xHis-tagged hFcγRIa (10256-H08H) were purchased from Sino Biologicals. C-terminally biotinylated human hFcγRIIIa-V158, hFcγRIIIb-NA1 and hFcγRIIIb-NA2 were produced: DNA sequences encoding the extracellular domain with an additional C-terminal tail containing respectively a linker, 10xHis-tag and AVI-tag (GLNDIFEAQKIEWHE) were codon-optimized by the online GeneArt Tools (Invitrogen), ordered at Integrated DNA Technologies and cloned into a pcDNA3.1 mammalian expression vector. The receptors were produced in human embryonic kidney (HEK293) Freestyle cells as described previously (Dekkers et al., 2016; Vink et al., 2013). Five days post-transfection cell supernatants were harvested, filtered through a 0.2 mm filter and isolated through affinity chromatography on an ÄKTAprime plus system (GE Life Sciences) using a His-trap column (GE Life Sciences) according to manufacturer's protocol. Subsequently, site-specific C-terminal *E. coli* biotin ligase (BirA)-mediated biotinylation was performed as described previously (Dekkers et al., 2018) with some adaptations: for biotinylation of 1 μM hFcγR 3.3 nM BirA ligase was added and Amicon Ultra centrifugal filter units (MWCO 10 kDa) (Merck, Millipore) were used to concentrate the sample and to remove unbound biotin.

2.6. Surface plasmon resonance imaging

SPRi measurements were performed on an IBIS MX96 (IBIS technologies) device as described previously (Dekkers et al., 2017a). All C-terminally biotinylated hFcγRs were spotted using a Continuous Flow Microspotter (Wasatch Microfluidics) onto a single SensEye G-streptavidin sensor (Ssens, 1–08–04–008) allowing for binding affinity measurements of each antibody to all hFcγR simultaneously on the IBIS MX96. The biotinylated hFcγRs were spotted in 3-fold dilutions, ranging from 30 nM to 1 nM for hFcγRIIa-H131, hFcγRIIIa-F158, hFcγRIIIa-V158, hFcγRIIIb-NA1 and hFcγRIIIb-NA2, and ranging from 10 nM to 0.3 nM for hFcγRIIa-R131 and hFcγRIIb in PBS supplemented with 0.075% Tween-80 (VWR, M126–100 ml), pH 7.4. Biotinylated anti-His mIgG1 (GenScript, A00613) was also spotted in this step in duplicate and 3-fold dilution, ranging from 30 nM to 1 nM. Subsequently, 25 nM His-tagged hFcγRIa was loaded onto the sensor before each antibody injection. Antibodies were then injected over the IBIS at 2-fold dilution series starting at 0.49 nM until 1000 nM in PBS + 0.075% Tween-80. The 6xHis-tagged EndoS was tested for interference of pre-existing 10xHis-tagged hFcγRIa immobilization to spotted anti-His (30-1 nM) by injecting EndoS over the sensor at 2-fold dilutions ranging from 50 nM to 1.56 nM (with 50 nM corresponding to the EndoS concentration in the highest [1000 nM] antibody flow) after hFcγRIa loading (25 nM). Regeneration after every sample was carried out with 10 nM Gly-HCl, pH 2.4. Calculation of the dissociation constant (K_D) was performed by equilibrium fitting to $R_{max} = 500$. In the case of anti-His spots, association and dissociation curves of His-tagged hFcγRIa were subtracted before calculation of IgG binding affinity using SPRINT 1.9.4.4 software (IBIS technologies). Analysis and calculation of all binding data was carried out with Scrubber software version 2 (Biologic Software) and Excel.

3. Results

3.1. Structural conservation of IgG subclasses and FcγRs between human and mice

First, we compared the conservation of the IgG-Fc domain within and between mouse and human subclasses. Alignment of the amino acid sequences of the CH2-CH3 Fc regions showed that all hIgG subclasses share substantial identity (91-94% homology and 96-99% similarity) (Table 1). Within mIgG subclasses, this identity appeared to be more subtle (62-82% homology and 80-91% similarity), with mIgG2a and mIgG2c being most identical, in line with the notion that these are likely to be allotypic variants of the same gene. The conservation between hIgG and mIgG subclasses was similar (61-68% homology and 77-86% similarity) as within the mouse subclasses.

We also compared the amino acid sequences of the FcγR extracellular domains within and between hFcγR and mFcγR. For hFcγRs, substantial homology within the hFcγRII and hFcγRIII families was found (Table 2). Within mouse classes only mFcγRIIb and mFcγRIII appeared to be homologous (93% homology and 95% similarity), similar to hFcγRIIb and hFcγRIIa, confirming the orthologous origin of these genes (Lejeune et al., 2019). Interspecies comparisons show considerable homology between mFcγRI and hFcγRIa (72% homology and 82% similarity), mFcγRIIb and hFcγRIIa/b/c (63-65% homology and 75-77% similarity), mFcγRIII and hFcγRIIa/b/c (61-62% homology and 73-75% similarity), and mFcγRIV and hFcγRIIIa/b (65-67% homology and 76-80% similarity). Taken together, based on the high homology between mice and humans for IgG subclasses and FcγRs, interspecies cross-interactions can be expected.

3.2. Interspecies cross-reactivity of mIgG subclasses to hFcγRs

To investigate the interspecies binding of monomeric mIgG

Table 1
Alignments of mIgG- and hIgG-Fc-CH2-CH3 amino acid sequences. Increasing degrees (in %) of homology (degree of identity between sequences, bold black) and similarity (degree of identity and positive substitutions between sequences, italic white) are indicated by increasing colour intensity (white to grey for homology; grey to black for similarity). Alignments were performed using the online blastp suite-2sequences tool (Altschul et al., 2005, 1997) and amino acid sequences were derived from UniProt.

		Human				Mouse				
		IgG1	IgG2	IgG3	IgG4	IgG1	IgG2a	IgG2b	IgG2c	IgG3
Human	IgG1		*99%*	*98%*	*98%*	*85%*	*79%*	*78%*	*80%*	*84%*
	IgG2	**94%**		*98%*	*98%*	*86%*	*79%*	*78%*	*80%*	*83%*
	IgG3	**94%**	**94%**		*96%*	*84%*	*77%*	*77%*	*79%*	*82%*
	IgG4	**94%**	**93%**	**91%**		*84%*	*79%*	*78%*	*80%*	*83%*
Mouse	IgG1	**65%**	**67%**	**66%**	**64%**		*83%*	*81%*	*80%*	*84%*
	IgG2a	**64%**	**65%**	**64%**	**64%**	**67%**		*88%*	*91%*	*82%*
	IgG2b	**62%**	**62%**	**61%**	**61%**	**62%**	**77%**		*89%*	*82%*
	IgG2c	**63%**	**62%**	**62%**	**63%**	**65%**	**82%**	**77%**		*80%*
	IgG3	**68%**	**68%**	**68%**	**65%**	**69%**	**71%**	**72%**	**69%**	

Similarity: *≤70%* | *71-80%* | *81-90%* | *91-100%*

Homology: ≤60% | 61-70% | 71-80% | 81-90% | 91-100%

Table 2
Alignments of mFcγR and hFcγR extracellular domain amino acid sequences. Increasing degrees (in %) of homology (degree of identity between sequences, bold black) and similarity (degree of identity and positive substitutions between sequences, italic white) are indicated by increasing colour intensity (white to grey for homology; grey to black for similarity). Alignments were performed using the online blastp suite-2sequences tool (Altschul et al., 2005, 1997) and amino acid sequences were derived from UniProt.

		Human						Mouse			
		FcγRIa	FcγRIIa	FcγRIIb	FcγRIIc	FcγRIIIa	FcγRIIIb	FcγRI	FcγRIIb	FcγRIII	FcγRIV
Human	FcγRIa		*65%*	*64%*	*63%*	*65%*	*65%*	*82%*	*67%*	*67%*	*62%*
	FcγRIIa	**46%**		*96%*	*95%*	*64%*	*65%*	*64%*	*75%*	*73%*	*65%*
	FcγRIIb	**47%**	**94%**		*100%*	*65%*	*66%*	*64%*	*77%*	*74%*	*67%*
	FcγRIIc	**46%**	**92%**	**100%**		*65%*	*66%*	*63%*	*77%*	*75%*	*66%*
	FcγRIIIa	**44%**	**51%**	**50%**	**50%**		*98%*	*60%*	*68%*	*66%*	*76%*
	FcγRIIIb	**46%**	**52%**	**51%**	**51%**	**97%**		*62%*	*68%*	*66%*	*80%*
Mouse	FcγRI	**72%**	**46%**	**47%**	**46%**	**44%**	**46%**		*44%*	*66%*	*61%*
	FcγRIIb	**45%**	**63%**	**65%**	**65%**	**51%**	**51%**	**29%**		*95%*	*63%*
	FcγRIII	**45%**	**61%**	**62%**	**61%**	**49%**	**50%**	**47%**	**93%**		*63%*
	FcγRIV	**44%**	**50%**	**51%**	**50%**	**65%**	**67%**	**41%**	**45%**	**46%**	

Similarity: *≤70%* | *71-80%* | *81-90%* | *91-100%*

Homology: ≤60% | 61-70% | 71-80% | 81-90% | 91-100%

subclasses towards hFcγRs, an SPRi-based multiplex biosensor platform was used where all different hFcγRs were immobilized through a C-terminal tag onto an SPR sensor. This system was generated using previously described well-characterized recombinant mIgG subclasses, hIgG1 and recombinant hFcγR classes (Dekkers et al., 2017b; Howie et al., 2016).

We first validated the SPRi system, injecting serially-diluted hIgG1 over the FcγR sensor, as hIgG1 is known to bind to all hFcγR classes with fairly defined affinities (Bruhns et al., 2009; Dekkers et al., 2017a). The resulting K_D values (Fig. 1a-b) were consistent with affinities described in the literature (Boesch et al., 2017; Bruhns et al., 2009) and those determined previously by our group (Dekkers et al., 2017a, 2017b).

We then repeated the procedure with monomeric (as confirmed by HPLC; Fig. S1) mIgG subclasses. Binding data (Fig. 1a-b) demonstrated that mIgG2a, mIgG2c and mIgG3 bound hFcγRIa in a similar high affinity range (3.6 ± 0.6 nM; 4.1 ± 0.9 nM; 9.9 ± 1.2 nM, respectively) as hIgG1 (4.1 ± 1.5 nM) (Fig. 1b). In addition, mIgG2b binds with two orders of magnitude lower affinity to hFcγRIa and mIgG1 does not bind. mIgG2a, mIgG2c, and mIgG2b (K_D for mIgG2b not calculable) bound with low affinity to hFcγRIIa irrespective of the H/R131 polymorphism. mIgG1 also bound with low affinity to hFcγRIIa-H131 (1.3 ± 0.5 μM). As expected, mIgG1 bound particularly strong to the hFcγRIIa-R131 variant (58.2 ± 14.4 nM), exceeding the affinity of hIgG1 for this receptor (0.5 ± 0.2 μM). Next to hFcγRIIa, mIgG1 also bound hFcγRIIb with a low affinity, which was also observed for mIgG2a, mIgG2b (K_D not calculable) and mIgG2c. Differential binding to polymorphic variants also occurred for the low affinity binding of mIgG2a and mIgG2c to hFcγRIIIa-V/F158, with slightly higher affinities towards the V158 variant (2.0 ± 0.4 μM and 2.6 ± 0.5 μM, respectively) compared to F158 (K_D not calculable). None of the mIgG subclasses bound to hFcγRIIIb. Overall, mIgG2a and mIgG2c showed very similar binding patterns, consistent with their substantial homology (Table 1).

3.3. Enzymatic glycan digestion of mIgG diminishes binding to most hFcγRs

To avoid undesired cross-reactivities, many researchers use EndoS to eliminate FcγR binding and thereby diminish background signals. As the efficacy of this approach has not been fully characterized for mIgG-hFcγR interactions, we deglycosylated all mIgG subclasses through enzymatic glycan digestion with recombinant EndoS (Fig. S2). The 6xHis-tagged EndoS, still present in the deglycosylated samples, did not interfere with pre-existing binding of 10xHis-tagged hFcγRIa to immobilized anti-His (30-1 nM) spots (Fig. S3). Deglycosylation of mIgG1 appeared to abolish binding to hFcγRIIa-H131 and hFcγRIIb and to diminish the only residual binding to hFcγRIIa-R131 with two orders of magnitude (from 58.2 ± 14.4 nM to 1.0 ± 0.2 μM) (Fig. 2a-b). Surprisingly, for mIgG2a and mIgG2c, binding to hFcγRIa was hardly

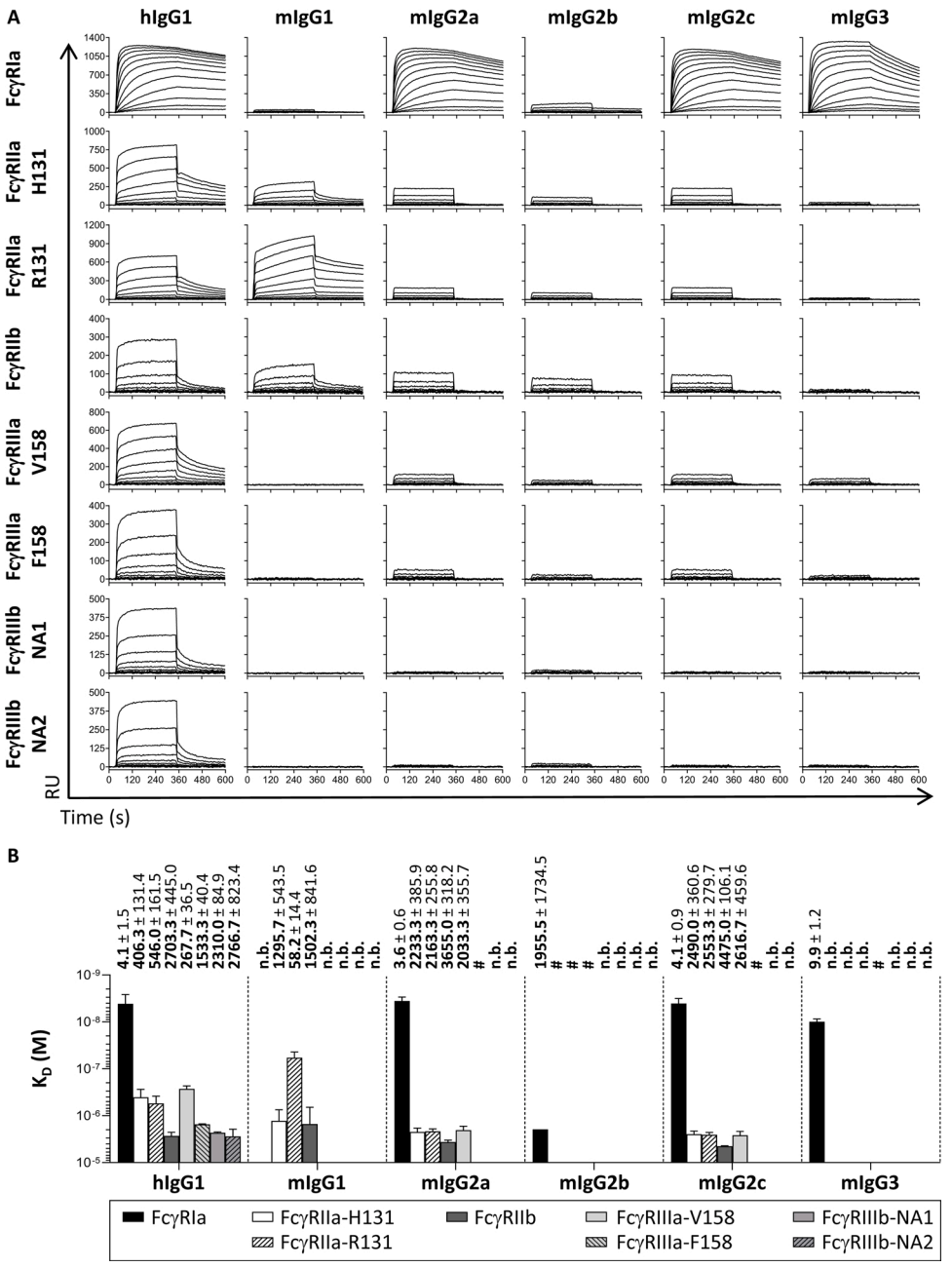

Fig. 1. Binding of mIgG subclasses to hFcγRs. (A) Representative sensorgrams showing binding of serial dilutions of each mIgG subclass (mIgG1, mIgG2a, mIgG2b, mIgG2c, mIgG3) to hFcγR classes (hFcγRIa, hFcγRIIa-H/R131, hFcγRIIb, hFcγRIIIa-V/F158, hFcγRIIIb-NA1/NA2). Depicted data are representative for three independent experiments where antibody binding was imaged in real-time and simultaneously to in duplo-spotted hFcγR classes at different densities (10 and 1 nM). Each line represents a specific IgG dilution and hIgG1 was used as positive control for hFcγR binding. (B) Quantified average K_D values (in M + standard error of the mean) of each mIgG subclass (mIgG1, mIgG2a, mIgG2b, mIgG2c, mIgG3) to hFcγR classes (hFcγRIa, hFcγRIIa-H/R131, hFcγRIIb, hFcγRIIIa-V/F158, hFcγRIIIb-NA1/NA2) as indicated in the legend. Exact K_D values are averages of three K_D values (in nM ± standard deviation) determined in three independent SPRi experiments and depicted above each bar. No binding events are indicated by n.b., and events when there was binding but too low to calculate a K_D value are indicated by #. The log scale on the y-axis is inversed.

affected by this treatment, while binding to the other receptors were reduced to very low levels after glycan digestion. Albeit a 4-fold reduction in affinity, still strong binding remained for mIgG3 to hFcγRIa after EndoS-mediated deglycosylation (from 9.9 ± 1.2 nM to 42.8 ± 4.9 nM). A complete disruption of binding to all hFcγR classes by EndoS treatment was only achieved for the weakest cross-reactive mIgG subclass: mIgG2b.

4. Discussion

Although fundamental basics on species-specific IgG-FcγR interactions have been studied extensively for both human and mouse (Boesch et al., 2017; Bruhns et al., 2009; Chan et al., 2016; Dekkers et al., 2017a, 2017b; Derebe et al., 2018), our knowledge on interspecies interactions have remained fragmented. However, this information is important to interpret results of animal models using hIgG and when using xenogeneic mAbs studying human material. Only recently, full profiles of binding reactivities of hIgG with mouse and macaque FcγR were published (Chan et al., 2016; Dekkers et al., 2017a; Derebe et al., 2018). Here, we extended this knowledge by providing for the first time detailed quantifiable information on cross-reactivity between the complete repertoire of mIgG (the most commonly used source of mAbs for research and diagnostics) and all hFcγR classes. Previous studies tackling this problem only reported relative affinities using incomplete hFcγR panels (Jönsson et al., 2011; Mancardi et al., 2013; van der Pol and van de Winkel, 1998) and/or incomplete mIgG panels (Miller et al., 1996).

The general ranking of mIgG affinity to hFcγR was mIgG2a = mIgG2c > mIgG1 > mIgG2b > mIgG3 and hFcγRIa > hFcγRIIa > hFcγRIIb > hFcγRIIIa, where hFcγRIIIb did not bind any mIgG. In some cases this binding was very efficient; for mIgG2a, mIgG2c and mIgG3 binding affinities to hFcγRIa on par with that of hIgG1. The fact that mIgG3 binds hFcγRIa is perhaps surprising as this subclass does not bind any mFcγR (Dekkers et al., 2017a) although it has been reported to bind with low

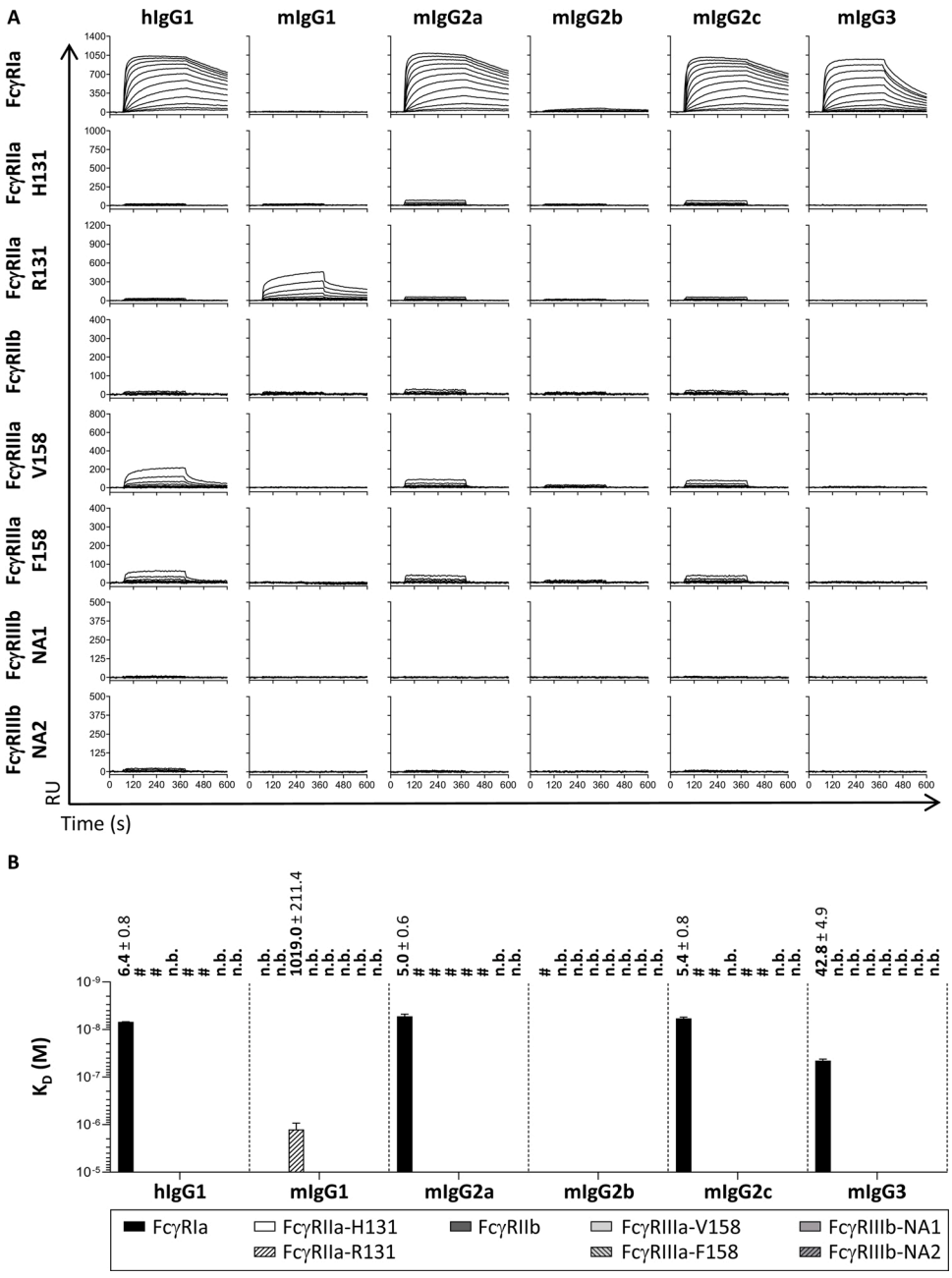

Fig. 2. Deglycosylation of mIgG through EndoS treatment decreases cross-reactivity to hFcγRs. (A) Representative sensorgrams showing binding of serial dilutions of each deglycosylated mIgG subclass (mIgG1, mIgG2a, mIgG2b, mIgG2c, mIgG3) to hFcγRs (hFcγRIa, hFcγRIIa-H/R131, hFcγRIIb, hFcγRIIIa-V/F158, hFcγRIIIb-NA1/NA2). Depicted data are representative for three independent experiments where antibody binding was imaged in real-time and simultaneously to in duplo-spotted hFcγRs at different densities (10 and 1 nM). Each line represents a specific IgG dilution and hIgG1 was used as positive control for hFcγR binding. (B) Quantified average K_D values (in M + standard error of the mean) of each EndoS deglycosylated mIgG subclass (mIgG1, mIgG2a, mIgG2b, mIgG2c, mIgG3) to hFcγRs (hFcγRIa, hFcγRIIa-H/R131, hFcγRIIb, hFcγRIIIa-V/F158, hFcγRIIIb-NA1/NA2) as indicated in the legend. Exact K_D values are averages of three K_D values (in nM ± standard deviation) determined in three independent SPRi experiments and depicted above each bar. No binding events are indicated by n.b., and events when there was binding but too low to calculate a K_D value are indicated by #. The log scale on the y-axis is inversed.

affinity to some mFcγRI allotypes (Gavin et al., 2000). However, the observed binding to hFcγRIa is in agreement with older data showing mIgG3 binding to human myeloid cells (Lubeck et al., 1985) and more recent work demonstrating binding of monomeric mIgG3 and immune complexes to hFcγRIa-transfected Chinese hamster ovary cells (Mancardi et al., 2013). This also makes mIgG3 less suitable for studies involving human myeloid cells than one might expect. We note that we chose an SPRi-based setup with C-terminally-immobilized FcγRs to determine IgG affinities in our study, an approach which was evaluated previously by our group (de Taeye et al., 2020; Dekkers et al., 2018, 2017a, 2017b). Also here, our reported affinity values correspond generally to previous findings, despite differential experimental setups that form an obvious source of variation.

Our findings are consistent with the well-known differential binding of mIgG1 to hFcγRIIa-H/R131, being the foundation for the "high responder" and "low responder" individuals in T-cell proliferation with peripheral blood mononuclear cells using mIgG1 anti-CD3 mAbs. This was later found to be caused by the affinity difference of hFcγRIIa-R131 (high responders) and hFcγRIIa-H131 (homozygotes were low responders) to mIgG1 (Parren et al., 1992; Tax et al., 1984, 1983; Warmerdam et al., 1991). The weak or lack of mIgG binding to hFcγRIII also has been reported previously (Jönsson et al., 2011; Miller et al., 1996; van der Pol and van de Winkel, 1998).

Next to the complete spectrum of exact affinity values, other novel findings we report are mIgG2c binding patterns and the binding behaviour of all mIgG subclasses towards hFcγRIIb and the hFcγRIIIa-V/F158 and hFcγRIIIb-NA1/NA2 polymorphic variants which have never been fully investigated. In addition, our data shows a clear side-by-side comparison on the relative strength of these interactions, and therefore their relative relevance for biological assays. A potential limitation of this study is the use of recombinant hFcγRs. As these were derived from HEK293 cells, this may result in slightly altered glycosylation compared to native equivalents on immune cells (Patel et al., 2018) or recombinant hFcγRs from other cellular production systems (Hayes et al., 2017).

However, as hFcγR glycosylation has been reported to be variable between donors (Patel et al., 2019, 2018; Roberts et al., 2020), and because we do not fully understand the complete significance of this variability yet, the question remains open whether and then how exactly this affects FcγR-IgG binding profiles.

IgG-Fc-CH2-CH3 amino acid sequence alignments did not give any indications of orthologous relations between IgG from mouse and human origin, which is perhaps to be expected as the IgG constant region genes have slightly different evolutionary origins. The human constant region locus seems to be the result of a complete duplication of a cluster containing two γ encoding genes, a single prototypic α and ε encoding constant regions (one of the resulting ε gene being a pseudogene). In mice, only a single cluster encodes for all four γ-constant regions, with a single ε and α encoding gene (D'Addabbo et al., 2011). Binding patterns, however, are more informative for interspecies comparisons; mIgG1 binding patterns showed some similarities with hIgG2 concerning differential binding to hFcγRIIa-H/R131 polymorphic variants (albeit reversed preference) and the absence of hFcγRIa and hFcγRIIIa/b binding (Boesch et al., 2017; Bruhns et al., 2009; Dekkers et al., 2017a). mIgG2a/c resembled the binding patterns of hIgG1 and hIgG3 to some extent, where hFcγRIa is bound with high affinity and hFcγRIIa/b and hFcγRIIIa/b with low affinity. However, the absence of hFcγRIIIb binding makes these mIgG subclasses diverge from hIgG1 and hIgG3. mIgG2b is unique as it binds all hFcγR classes with extremely low affinity, except for no detectable binding to hFcγRIIIb. mIgG3 binding patterns also cannot be compared to any hIgG subclass since mIgG3 only showed high affinity binding to hFcγRIa which is not observed for any hIgG subclass.

Antibody deglycosylation with EndoS is a simple and useful method to avoid undesired background due to binding to FcγR and has been applied in *in vivo* animal models (Albert et al., 2008; Collin et al., 2008; Gao et al., 2015; Tradtrantip et al., 2013) and *in vitro* human studies (Lood et al., 2012; Lux et al., 2013; Tradtrantip et al., 2013) for both research and diagnostic purposes. It is well known that deglycosylation of hIgG abrogates binding to most hFcγRs, but with residual binding to hFcγRIa with reduced affinity (Lux et al., 2013). Our data demonstrate that Fc-glycan digestion of mIgG results in decreased interspecies cross-reactivity to the low-affinity hFcγRs. Remarkably, this had no marked effect on the high affinity binding to hFcγRIa by mIgG2a/c and mIgG3. Deglycosylated mIgG1 still reacted with moderate affinity with hFcγRIIa-R131, leaving deglycosylated mIgG2b being the only subclass not reacting with any hFcγR class. Current useful antibodies for diagnostics and research, that are not of this subclass, can potentially be class-switched by recently developed CRISPR/HDR genomic engineering techniques (van der Schoot et al., 2019), or cloned and expressed recombinantly (Howie et al., 2016).

In conclusion, mIgG subclasses have the ability to bind hFcγR classes and in some cases very efficiently. The exact affinity values reported in this study give an extensive overview and fill the gap in literature concerning this cross-reactivity. In addition, we also show the potential perils of using EndoS for most mIgG subclasses to eliminate background binding to hFcγR. However, the data also provide a simple solution to this problem: by using deglycosylated mIgG2b cross-reactivity is eliminated. Altogether, these data suggest mIgG generally have similar binding patterns as hIgG have to hFcγR which should be taken into consideration for application in a human context.

Author contributions

A.R.T. performed amino acid alignment studies. A.R.T. and A.E.H.B. performed SPRi experiments. A.E.H.B. analysed SPRi data and calculated K_D values. S.N.L.T., J.C.Z. and H.L.H. developed and/or produced anti-K mIgG subclasses. S.W.d.T. produced anti-Rhesus D hIgG1. N.I.L.D. performed HPLC tests. G.P.B. produced recombinant EndoS for IgG deglycosylation purposes. A.R.T. deglycosylated IgG formulations, performed SDS-PAGE experiments, cloned hFcγR-encoding constructs and produced the hFcγR classes. G.B., J.Y.M. and W.J.E.v.E performed site-specific biotinylation of the hFcγR classes. G.V. supervised the project. A.R.T. and G.V. designed all experiments and wrote the manuscript which was critically reviewed by all co-authors.

Funding

This work was funded by Landsteiner Foundation for Blood Transfusion Research (grant number 1527).

Declaration of Competing Interest

The authors report no declarations of interest.

Acknowledgements

The authors thank Maximilian Brinkhaus and Thijs van Osch for their help with SDS-PAGE experiments.

Appendix A. Supplementary data

Supplementary material related to this article can be found, in the online version, at doi:https://doi.org/10.1016/j.molimm.2020.08.015.

References

Albert, H., Collin, M., Dudziak, D., Ravetch, J.V., Nimmerjahn, F., 2008. In vivo enzymatic modulation of IgG glycosylation inhibits autoimmune disease in an IgG subclass-dependent manner. Proc. Natl. Acad. Sci. 105, 15005–15009. https://doi.org/10.1073/pnas.0808248105.

Altschul, S.F., Madden, T.L., Schäffer, A.A., Zhang, J., Zhang, Z., Miller, W., Lipman, D.J., 1997. Gapped BLAST and PSI-BLAST: a new generation of protein database search programs. Nucleic Acids Res. 25, 3389–3402. https://doi.org/10.1093/nar/25.17.3389.

Altschul, S.F., Wootton, J.C., Gertz, E.M., Agarwala, R., Morgulis, A., Schäffer, A.A., Yu, Y.-K., 2005. Protein database searches using compositionally adjusted substitution matrices. FEBS J. 272, 5101–5109. https://doi.org/10.1111/j.1742-4658.2005.04945.x.

Boesch, A.W., Miles, A.R., Chan, Y.N., Osei-Owusu, N.Y., Ackerman, M.E., 2017. IgG Fc variant cross-reactivity between human and rhesus macaque FcγRs. MAbs 9, 455–465. https://doi.org/10.1080/19420862.2016.1274845.

Bruggeman, C.W., Dekkers, G., Bentlage, A.E.H., Treffers, L.W., Nagelkerke, S.Q., Lissenberg-Thunnissen, S., Koeleman, C.A.M., Wuhrer, M., van den Berg, T.K., Rispens, T., Vidarsson, G., Kuijpers, T.W., 2017. Enhanced Effector Functions Due to Antibody Defucosylation Depend on the Effector Cell Fcγ Receptor Profile. J. Immunol. 199, 204–211. https://doi.org/10.4049/jimmunol.1700116.

Bruhns, P., 2012. Properties of mouse and human IgG receptors and their contribution to disease models. Blood 119, 5640–5649. https://doi.org/10.1182/blood-2012-01-380121.

Bruhns, P., Iannascoli, B., England, P., Mancardi, D.A., Fernandez, N., Jorieux, S., Daëron, M., 2009. Specificity and affinity of human Fcgamma receptors and their polymorphic variants for human IgG subclasses. Blood 113, 3716–3725. https://doi.org/10.1182/blood-2008-09-179754.

Candiano, G., Bruschi, M., Musante, L., Santucci, L., Ghiggeri, G.M., Carnemolla, B., Orecchia, P., Zardi, L., Righetti, P.G., 2004. Blue silver: A very sensitive colloidal Coomassie G-250 staining for proteome analysis, pp. 1327–1333. https://doi.org/10.1002/elps.200305844.

Chan, Y.N., Boesch, A.W., Osei-Owusu, N.Y., Emileh, A., Crowley, A.R., Cocklin, S.L., Finstad, S.L., Linde, C.H., Howell, R.A., Zentner, I., Cocklin, S., Miles, A.R., Eckman, J.W., Alter, G., Schmitz, J.E., Ackerman, M.E., 2016. IgG Binding Characteristics of Rhesus Macaque FcγR. J. Immunol. 197, 2936–2947. https://doi.org/10.4049/jimmunol.1502252.

Collin, M., Olsén, A., 2001. EndoS, a novel secreted protein from Streptococcus pyogenes with endoglycosidase activity on human IgG. EMBO J. 20, 3046–3055. https://doi.org/10.1093/emboj/20.12.3046.

Collin, M., Shannon, O., Björck, L., 2008. IgG glycan hydrolysis by a bacterial enzyme as a therapy against autoimmune conditions. Proc. Natl. Acad. Sci. 105, 4265–4270. https://doi.org/10.1073/pnas.0711271105.

D'Addabbo, P., Scascitelli, M., Giambra, V., Rocchi, M., Frezza, D., 2011. Position and sequence conservation in Amniota of polymorphic enhancer HS1.2 within the palindrome of IgH 3'Regulatory Region. BMC Evol. Biol. 11, 71. https://doi.org/10.1186/1471-2148-11-71.

de Taeye, S.W., Bentlage, A.E.H., Mebius, M.M., Meesters, J.I., Lissenberg-Thunnissen, S., Falck, D., Sénard, T., Salehi, N., Wuhrer, M., Schuurman, J., Labrijn, A.F., Rispens, T., Vidarsson, G., 2020. FcγR Binding and ADCC Activity of Human IgG Allotypes. Front. Immunol.

de Taeye, S.W., Rispens, T., Vidarsson, G., 2019. The Ligands for Human IgG and Their Effector Functions. Antibodies 8, 30. https://doi.org/10.3390/antib8020030.

Dekkers, G., Bentlage, A.E.H., Plomp, R., Visser, R., Koeleman, C.A.M., Beentjes, A., Mok, J.Y., van Esch, W.J.E., Wuhrer, M., Rispens, T., Vidarsson, G., 2018. Conserved FcγR- glycan discriminates between fucosylated and afucosylated IgG in humans and mice. Mol. Immunol. 94, 54–60. https://doi.org/10.1016/j.molimm.2017.12.006.

Dekkers, G., Plomp, R., Koeleman, C.A.M., Visser, R., Von Horsten, H.H., Sandig, V., Rispens, T., Wuhrer, M., Vidarsson, G., 2016. Multi-level glyco-engineering techniques to generate IgG with defined Fc-glycans. Sci. Rep. 6, 1–12. https://doi.org/10.1038/srep36964.

Dekkers, G., Bentlage, A.E.H., Stegmann, T.C., Howie, H.L., Lissenberg-Thunnissen, S., Zimring, J., Rispens, T., Vidarsson, G., 2017a. Affinity of human IgG subclasses to mouse Fc gamma receptors. MAbs 9, 767–773. https://doi.org/10.1080/19420862.2017.1323159.

Dekkers, G., Treffers, L., Plomp, R., Bentlage, A.E.H., Boer, M. de, Koeleman, C.A.M., Lissenberg-Thunnissen, S.N., Visser, R., Brouwer, M., Mok, J.Y., Matlung, H., van den Berg, T.K., van Esch, W.J.E., Kuijpers, T.W., Wouters, D., Rispens, T., Wuhrer, M., Vidarsson, G., 2017b. Decoding the human immunoglobulin G-glycan repertoire reveals a spectrum of Fc-receptor- and complement-mediated-effector activities. Front. Immunol. 8 https://doi.org/10.3389/fimmu.2017.00877.

Derebe, M.G., Nanjunda, R.K., Gilliland, G.L., Lacy, E.R., Chiu, M.L., 2018. Human IgG subclass cross-species reactivity to mouse and cynomolgus monkey Fcγ receptors. Immunol. Lett. 197, 1–8. https://doi.org/10.1016/j.imlet.2018.02.006.

Falconer, D.J., Subedi, G.P., Marcella, A.M., Barb, A.W., 2018. Antibody Fucosylation Lowers the FcγRIIIa/CD16a Affinity by Limiting the Conformations Sampled by the N162-Glycan. ACS Chem. Biol. 13, 2179–2189. https://doi.org/10.1021/acschembio.8b00342.

Feige, M.J., Nath, S., Catharino, S.R., Weinfurtner, D., Steinbacher, S., Buchner, J., 2009. Structure of the Murine Unglycosylated IgG1 Fc Fragment. J. Mol. Biol. 391, 599–608. https://doi.org/10.1016/j.jmb.2009.06.048.

Ferrara, C., Grau, S., Jager, C., Sondermann, P., Brunker, P., Waldhauer, I., Hennig, M., Ruf, A., Rufer, A.C., Stihle, M., Umana, P., Benz, J., 2011. Unique carbohydrate-carbohydrate interactions are required for high affinity binding between Fc RIII and antibodies lacking core fucose. Proc. Natl. Acad. Sci. 108, 12669–12674. https://doi.org/10.1073/pnas.1108455108.

Gao, P., Pinkston, K.L., Wilganowski, N., Robinson, H., Azhdarinia, A., Zhu, B., Sevick-Muraca, E.M., Harvey, B.R., 2015. Deglycosylation of mAb by EndoS for Improved Molecular Imaging. Mol. Imaging Biol. 17, 195–203. https://doi.org/10.1007/s11307-014-0781-9.

Gavin, A., Leiter, E., Hogarth, P.M., 2000. Mouse FcγRI: Identification and functional characterization of five new alleles. Immunogenetics 51, 206–211. https://doi.org/10.1007/s002510050033.

Hayes, J.M., Frostell, A., Karlsson, R., Mu, S., Míllan, S., Pauers, M., Reuss, F., Cosgrave, E.F., Anneren, C., Davey, G.P., Rudd, P.M., 2017. Identification of Fc Gamma Receptor Glycoforms That Produce Differential Binding Kinetics for Rituximab, pp. 1770–1788. https://doi.org/10.1074/mcp.M117.066944.

Hogarth, P.M., Pietersz, G.A., 2012. Fc receptor-targeted therapies for the treatment of inflammation, cancer and beyond. Nat. Rev. Drug Discov. 11, 311–331. https://doi.org/10.1038/nrd2909.

Howie, H.L., Delaney, M., Wang, X., Er, L.S., Vidarsson, G., Stegmann, T.C., Kapp, L., Lebedev, J.N., Wu, Y., AuBuchon, J.P., Zimring, J.C., 2016. Serological blind spots for variants of human IgG3 and IgG4 by a commonly used anti-immunoglobulin reagent. Transfusion 56, 2953–2962. https://doi.org/10.1111/trf.13812.

Jones, D.H., Looney, R.J., Anderson, C.L., 1985. Two distinct classes of IgG Fc receptors on a human monocyte line (U937) defined by differences in binding of murine IgG subclasses at low ionic strength. J. Immunol. 135, 3348–3353.

Jönsson, F., Mancardi, D.A., Kita, Y., Karasuyama, H., Iannascoli, B., Van Rooijen, N., Shimizu, T., Daëron, M., Bruhns, P., 2011. Mouse and human neutrophils induce anaphylaxis. J. Clin. Invest. 121, 1484–1496. https://doi.org/10.1172/JCI45232.

Kipps, T.J., Parham, P., Punt, J., Herzenberg, L.A., 1985. Importance of immunoglobulin isotype in human antibody-dependent, cell-mediated cytotoxicity directed by murine monoclonal antibodies. J. Exp. Med. 161, 1–17. https://doi.org/10.1084/jem.161.1.1.

Kurlander, R.J., 1983. Blockade of Fc receptor-mediated binding to U-937 cells by murine monoclonal antibodies directed against a variety of surface antigens. J. Immunol. 131, 140–147.

Lejeune, J., Brachet, G., Watier, H., 2019. Evolutionary Story of the Low/Medium-Affinity IgG Fc Receptor Gene Cluster. Front. Immunol. 10, 1297 https://doi.org/10.3389/fimmu.2019.01297.

Lippold, S., Nicolardi, S., Dominguez-Vega, E., Heidenreich, A.-K., Vidarsson, G., Reusch, D., Haberger, M., Wuhrer, M., Falck, D., 2019. Glycoform-resolved FcRIIIa affinity chromatography-mass spectrometry. MAbs 11, 1191–1196. https://doi.org/10.1080/19420862.2019.1636602.

Liu, L., Prudden, A.R., Bosman, G.P., Boons, G.-J., 2017. Improved isolation and characterization procedure of sialylglycopeptide from egg yolk powder. Carbohydr. Res. 452, 122–128. https://doi.org/10.1016/j.carres.2017.10.001.

Lood, C., Allhorn, M., Lood, R., Gullstrand, B., Olin, A.I., Ronnblom, L., Truedsson, L., Collin, M., Bengtsson, A.A., 2012. IgG glycan hydrolysis by endoglycosidase S diminishes the proinflammatory properties of immune complexes from patients with systemic lupus erythematosus: a possible new treatment? Arthritis Rheum. 64, 2698–2706. https://doi.org/10.1002/art.34454.

Lubeck, M.D., Steplewski, Z., Baglia, F., Klein, M.H., Dorrington, K.J., Koprowski, H., 1985. The interaction of murine IgG subclass proteins with human monocyte Fc receptors. J. Immunol. 135, 1299–1304.

Lux, A., Yu, X., Scanlan, C.N., Nimmerjahn, F., 2013. Impact of Immune Complex Size and Glycosylation on IgG Binding to Human FcγRs. J. Immunol. 190, 4315–4323. https://doi.org/10.4049/jimmunol.1200501.

MacIntyre, E.A., Roberts, P.J., Abdul-Gaffar, R., O'Flynn, K., Pilkington, G.R., Farace, F., Morgan, J., Linch, D.C., 1988. Mechanism of human monocyte activation via the 40-kDa Fc receptor for IgG. J. Immunol. 141, 4333–4343.

MacIntyre, E.A., Roberts, P.J., Jones, M., Van der Schoot, C.E., Favalaro, E.J., Tidman, N., Linch, D.C., 1989. Activation of human monocytes occurs on cross-linking monocytic antigens to an Fc receptor. J. Immunol. 142, 2377–2383.

Mancardi, D.A., Albanesi, M., Jönsson, F., Iannascoli, B., Van Rooijen, N., Kang, X., England, P., Daëron, M., Bruhns, P., 2013. The high-affinity human IgG receptor FcγRI (CD64) promotes IgG-mediated inflammation, anaphylaxis, and antitumor immunotherapy. Blood 121, 1563–1573. https://doi.org/10.1182/blood-2012-07-442541.

Martin, R.M., Brady, J.L., Lew, A.M., 1998. The need for IgG2c specific antiserum when isotyping antibodies from C57BL/6 and NOD mice. J. Immunol. Methods 212, 187–192. https://doi.org/10.1016/s0022-1759(98)00015-5.

Meinderts, S.M., Oldenborg, P.-A., Beuger, B.M., Klei, T.R.L., Johansson, J., Kuijpers, T. W., Matozaki, T., Huisman, E.J., de Haas, M., van den Berg, T.K., van Bruggen, R., 2017. Human and murine splenic neutrophils are potent phagocytes of IgG-opsonized red blood cells. Blood Adv. 1, 875–886. https://doi.org/10.1182/bloodadvances.2017004671.

Miller, K.L., Duchemin, A.M., Anderson, C.L., 1996. A novel role for the Fc receptor gamma subunit: enhancement of Fc gamma R ligand affinity. J. Exp. Med. 183, 2227–2233. https://doi.org/10.1084/jem.183.5.2227.

Parren, P.W., Warmerdam, P.A., Boeije, L.C., Capel, P.J., van de Winkel, J.G., Aarden, L. A., 1992. Characterization of IgG FcR-mediated proliferation of human T cells induced by mouse and human anti-CD3 monoclonal antibodies. Identification of a functional polymorphism to human IgG2 anti-CD3. J. Immunol. 148, 695–701.

Patel, K.R., Nott, J.D., Barb, A.W., 2019. Primary Human Natural Killer Cells Retain Proinflammatory IgG1 at the Cell Surface and Express CD16a Glycoforms with Donor-dependent Variability. Mol. Cell. Proteomics 18, 2178–2190. https://doi.org/10.1074/mcp.RA119.001607.

Patel, K.R., Roberts, J.T., Subedi, G.P., Barb, A.W., 2018. Restricted processing of CD16a/Fc gamma receptor IIIa N-glycans from primary human NK cells impacts structure and function. J. Biol. Chem. 293, 3477–3489. https://doi.org/10.1074/jbc.RA117.001207.

Roberts, J.T., Patel, K.R., Barb, A.W., 2020. Site-specific N-glycan Analysis of Antibody-binding Fc γ Receptors from Primary Human Monocytes. Mol. Cell. Proteomics 19, 362–374. https://doi.org/10.1074/mcp.RA119.001733.

Saeland, E., Royen, A. van, Hendriksen, K., Vilé-Weekhout, H., Rijkers, G.T., Sanders, L. A.M., Winkel, J.G.J. van de, 2001. Human C-reactive protein does not bind to fcγRIIa on phagocyti cells. J. Clin. Invest. 107, 641. https://doi.org/10.1172/JCI12418.

Subedi, G.P., Barb, A.W., 2018. CD16a with oligomannose-type N-glycans is the only "low-affinity" Fc γ receptor that binds the IgG crystallizable fragment with high affinity in vitro. J. Biol. Chem. 293, 16842–16850. https://doi.org/10.1074/jbc.RA118.004998.

Subedi, G.P., Barb, A.W., 2016. The immunoglobulin G1 N-glycan composition affects binding to each low affinity Fc γ receptor. MAbs 8, 1512–1524. https://doi.org/10.1080/19420862.2016.1218586.

Tax, W.J., Hermes, F.F., Willems, R.W., Capel, P.J., Koene, R.A., 1984. Fc receptors for mouse IgG1 on human monocytes: polymorphism and role in antibody-induced T cell proliferation. J. Immunol. 133, 1185–1189.

Tax, W.J., Willems, H.W., Reekers, P.P., Capel, P.J., Koene, R.A., 1983. Polymorphism in mitogenic effect of IgG1 monoclonal antibodies against T3 antigen on human T cells. Nature 304, 445–447. https://doi.org/10.1038/304445a0.

Temming, A.R., de Taeye, S.W., de Graaf, E.L., de Neef, L.A., Dekkers, G., Bruggeman, C. W., Koers, J., Ligthart, P., Nagelkerke, S.Q., Zimring, J.C., Kuijpers, T.W., Wuhrer, M., Rispens, T., Vidarsson, G., 2019. Functional attributes of antibodies, effector cells, and target cells affecting NK cell–mediated antibody-dependent cellular cytotoxicity. J. Immunol. 203 (12), 3126–3135. https://doi.org/10.4049/jimmunol.1900985.

Tradtrantip, L., Ratelade, J., Zhang, H., Verkman, A.S., 2013. Enzymatic deglycosylation converts pathogenic neuromyelitis optica anti-aquaporin-4 immunoglobulin G into therapeutic antibody. Ann. Neurol. 73, 77–85. https://doi.org/10.1002/ana.23741.

van der Pol, W.-L., van de Winkel, J.G.J., 1998. IgG receptor polymorphisms: risk factors for disease. Immunogenetics 48, 222–232. https://doi.org/10.1007/s002510050426.

van der Schoot, J.M.S., Fennemann, F.L., Valente, M., Dolen, Y., Hagemans, I.M., Becker, A.M.D., Le Gall, C.M., van Dalen, D., Cevirgel, A., van Bruggen, J.A.C., Engelfriet, M., Caval, T., Bentlage, A.E.H., Fransen, M.F., Nederend, M., Leusen, J.H. W., Heck, A.J.R., Vidarsson, G., Figdor, C.G., Verdoes, M., Scheeren, F.A., 2019. Functional diversification of hybridoma-produced antibodies by CRISPR/HDR genomic engineering. Sci. Adv. 5, eaaw1822 https://doi.org/10.1126/sciadv.aaw1822.

Vidarsson, G., Dekkers, G., Rispens, T., 2014. IgG subclasses and allotypes: from structure to effector functions. Front. Immunol. 5, 520 https://doi.org/10.3389/fimmu.2014.00520.

Vink, T., Dickmann, M., Roza, M., Reitsma, J.-J., Jong, R., 2013. A simple, robust and highly efficient transient expression system for producing antibodies. Methods 65. https://doi.org/10.1016/j.ymeth.2013.07.018.

Warmerdam, P.A., van de Winkel, J.G., Vlug, A., Westerdaal, N.A., Capel, P.J., 1991. A single amino acid in the second Ig-like domain of the human Fc gamma receptor II is critical for human IgG2 binding. J. Immunol. 147, 1338–1343.